DUST DEVIL ORIENTATION AND MARTIAN SURFACE WINDS. L. K. Tamppari[1], V. Ochoa[2], V. Sun[1]. [1]Jet Propulsion Laboratory/California Institute of Technology, Pasadena, CA, USA. [2]Arizona State University, Phoenix, AZ, USA.

Introduction: Dust devils tracks (DDTs) are seen over much of the Martian surface [1]. They are thought to be caused by surface-atmosphere temperature contrast causing convective vortices that lift (typically, higher albedo) dust, leaving behind a relatively dark track. A few years prior to the Phoenix north polar lander mission (2008; landing location 68.22°N, 234.25°E, [2]), the supposition was that dust devils would not occur at such high latitudes given the presumed smaller surface-atmosphere temperature contrast. However, many dust devil tracks were seen using MGS MOC data in the 65-72N latitude band of Mars [3], which included the four potential landing sites for the Phoenix lander. Once Phoenix landed, dust devils were observed nearby with the Solid State Imager [4] and pressure vortices consistent with passing dust devils ("dustless" devils) were observed via their characteristic pressure signature using Phoenix meteorology pressure sensor [5,6]. This study extends in time the catalog of dust devil tracks using more than 500 images from the Mars Reconnaissance Orbiter's Context Camera (CTX,[7]), and uses the dust devil track orientation as a proxy for the wind direction for comparison of the winds detected by the Phoenix Telltale wind indicator [8].

Data and Methods: *DDT location and orientation.* MRO CTX images in the 65-72 N latitude band were examined to find and catalog DDTs. ArcMap, a geographic information system, was used to view the georeferenced and map-projected images, to trace DDTs, and determine their longitudes and directions (North corresponds to 0º and East corresponds to 90º). Most of the images that were analyzed were taken during Mars Year 29 (2008-2009), overlapping with the Phoenix mission (May-November, 2008). Over 9,500 visible dust devil tracks were individually traced.

Wind speed and direction. It is desirable to know the wind direction associated with the DDTs. However, DDTs are an ambiguous record of wind direction, since DDT oriented at 0º or 180º could indicate winds from either North or South. Thus, wind speed and direction data from the Telltale wind indicator throughout the 151-sol Phoenix mission were examined. Hundreds of wind measurements were made every sol beginning on Sol 3 until Sol 151, resulting in more than a total of 7,000 wind measurements at various times of the day during the mission.

Results: *DDT location and orientation.* DDTs were found at all longitudes in the 65-72N band (Fig. 1), although some octants had a higher concentration of DDTs than others. The octant with the largest number of DDTs was L-7 (270-315E), which had 3,403 DDTs. The octant with the fewest DDTs was L-3 (90-135E) with only 26. Each octant's DDTs also in orientation. For example, in L-6 (225-270E), DDTs are primarily north-south and east-west oriented. But in L-7 (270-315E), one 45-degree bin to the East, DDTs are primarily northwest-southeast oriented.

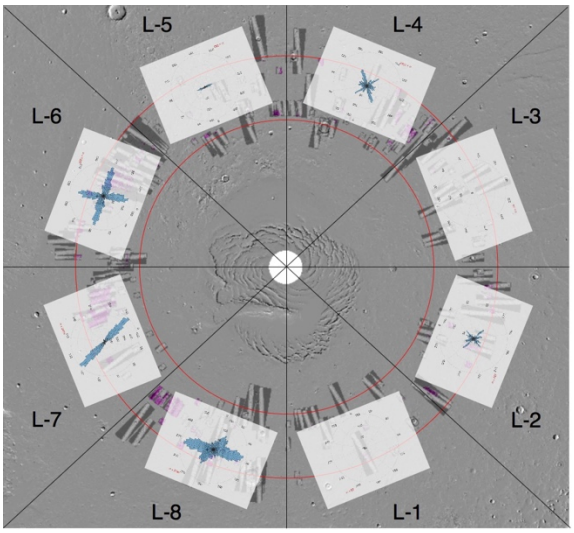

Fig. 1: Polar projection of dust devil tracks found in the 65-72N band (red circles) of Mars. Longitudes sectors are separated into eight 45-degree bins. L-1 is 0-45º E, L-2 is 45-90º E, etc. CTX images are represented by dark grey rectangular boxes with white strips inside. Pink shading within these boxes indicates DDTs. Overlain are N-S-aligned rose diagrams showing the number of DDTs and their orientations for that octant.

Dust devil track changes. A time series of CTX images that overlapped the Phoenix landing site octant and mission duration were studied to search for occurrence and disappearance of DDTs. Two CTX images that include the Phoenix landing site stood out: P22_009725_2484 and B01_009857_2484, which will hereafter be referred to as Image 1 and Image 2, respectively (Fig. 2, left and right, respectively). Image 1 was taken on 2008-08-23 (Sol 89) and had no visible DDTs and Image 2, taken only 9 sols later on 2008-09-02 (Sol 98), had 109 DDTs. Dust devils formed and left tracks sometime between the acquisition dates of these two CTX images. The DDTs occur with two distinct orientations: north-northeast to south-southwest, and northwest to southeast (Fig. 3).

Comparison of DDTs to Phoenix wind data. Using contemporaneous Phoenix Telltale wind measurements, the directions of the dust devils that left tracks between Phoenix Sols 89-98 were determined. Phoenix took 726 wind measurements between Sols 89-98. On Sol 93, Phoenix saw an increase in dust devil activity [8] and measured winds coming from the southeast (~135º), closely matching one DDT orientation mode. On Sol 94, most of the wind data shows the direction having a value of about 20º which corresponds to winds coming from the north-northeast towards the south-southwest, closely matching the other DDT orientation mode (Fig. 3).

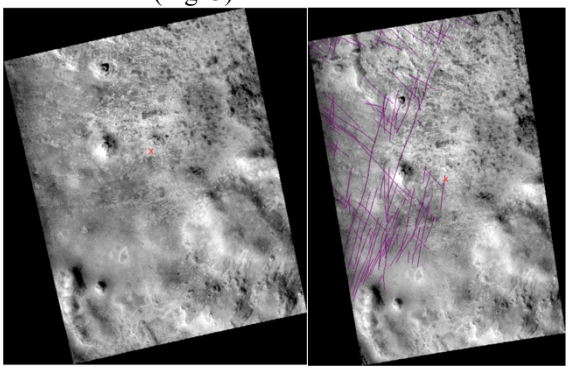

Fig. 2: (Left) CTX image ID P22_009725_2484 acquired on 2008-08-23 (Sol 89). (Right) CTX image B01_009857_2484 acquired on 2008-09-02 (Sol 98) with DDTs in purple. Phoenix landing site marked with a red 'x'.

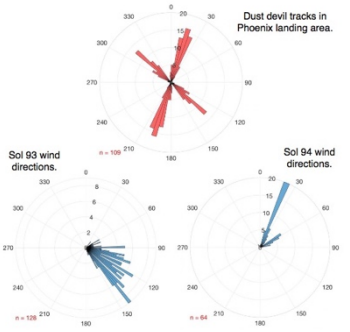

Fig. 3 (Top) Rose diagram of dust devil track orientation from image B01_009857_2484. (Bottom-left) Wind direction for Sol 93 of Phoenix mission. (Bottom-right) Wind direction for Sol 94 of Phoenix mission.

Discussion: *DDT location and orientation.* A larger number of DDTs appear to occur between 225-360º E (Fig. 1; L-6 through L-8). This may be due to the fact that there are more CTX images in those octants and therefore a higher chance that a DDTs will be found. Alternatively, different surface materials could be present in this area allowing dust devil tracks to appear more easily; only 14% of dust devils may leave behind tracks [9]. The area within that longitude may also be more conducive to DDT formation as it is a known storm track region [10].

Comparison of DDTs to Phoenix wind data. The observed DDTs that occurred between sols 89-98 are most likely associated with a passing low pressure system. On sol 93-95, the Phoenix pressure sensor measured a pressure drop associated with such a passing system [11]. Examination of the Telltale wind measurements for these days show that winds speeds were primarily > 8 m/s (Fig. 4), whereas, typically, wind speeds were < 8 m/s. In fact, only 84 of the 726 measurements taken over sols 89-98 exceeded 8 m/s, and 82 of these 84 measurements occurred during sols 93-94. This indicates that, for the Phoenix vicinity, higher velocities may be necessary to drive dust devils that leave behind tracks.

Conclusions: DDTs occurring in the 65-72N latitude band during MY29 were cataloged using CTX data. DDTs were found in all longitudes, but were more commonly found between 225 -360º E. Although this region is a known storm track region which may be responsible for more DDTs, this may also be an observation bias due to the greater CTX coverage. Images which included the Phoenix lander and were taken during the Phoenix mission were examined to search for changes. A significant number of DDTs were observed to occur between sols 89-98. A low-p system passed over Phoenix on sols 93-95 and increased winds (>8 m/s) were observed on sols 93-94. The orientations of the DDTs compare well to the higher-speed wind directions measured on sols 93-94.

These results demonstrate for the first time that the correlation of dust devil tracks, detected from orbital imagery, with in-situ surface weather measurements can help constrain formation conditions for Martian dust devil tracks.

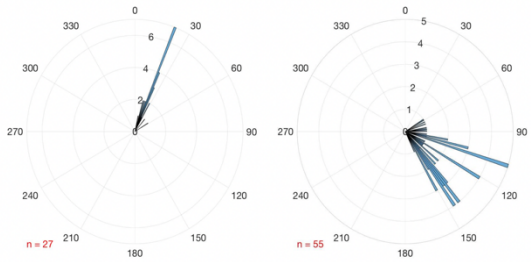

Fig. 4: (Left) The number of wind measurements > 8 m/s per directional bin for Sol 93; total n=27. (Right) Same for Sol 94. Total n=55.

References: [1] Hausmann *et al.* (2019) *LPSC 50 #2132.* [2] Smith *et al.* (2009) *Science* **325**(5936). [3] Drake *et al.* (2006) *GRL* **33**. [4] Lemmon *et al.* (2008) *LPSC 39 #2156.* [5] Ellehoj *et al.* (2010) *JGR* **115**(E00E16). [6] Taylor *et al.* (2008) *JGR* **113**(E00A10). [7] Malin *et al.* (2007) *JGR* **112**(E05S04). [8] Holstein-Rathlou *et al.* (2010) *JGR* **115**(E00E18). [9] Cantor *et al.* (2006) *JGR* **111**(E12002). [10] Tamppari *et al.* (2000) *JGR* **105**(E001133). [11] Taylor *et al.* (2010) *JGR* **115**(E00E15).